Analysis of the Operational Modes of the Phase Modulated LLC Resonant Converter

Umme Mumtahina
Central Queensland University
Rockhampton, Australia
u.mumtahina@cqu.edu.au

Sanath Alahakoon
Central Queensland University
Rockhampton, Australia
s.alahakoon@cqu.edu.au

Peter Wolfs
Central Queensland University
Rockhampton, Australia
p.wolfs@cqu.edu.au

***Abstract*—This paper presents the steady state analysis of the full bridge LLC resonant converter. Six switching stages are found due to the odd symmetry. Once the information about state variables are at hand, state plane trajectory can be constructed for each state. In this paper a detailed analysis has been presented for phase modulated LLC resonant converter to predict the resonant voltage and current waveforms of the operational modes. For these operational modes, two dimensional state plane trajectories are also observed. A design guideline has been proposed to assess which modes are practically useful and will have the highest efficiency.**

Keywords—Operational modes, Phase Modulation, LLC resonant converter, State plane trajectory.

I. INTRODUCTION

Resonant converters have been extensively researched since 1970s [1]. Two most popular topologies are the series and the parallel resonant converters [2,3]. These resonant converters have highest efficiency at or near the resonant region. In this region they will have lower conduction losses. Series resonant converters can have high efficiency but it have some disadvantages [4]. The LLC resonant converter offers improvements in these areas and has quickly become one of the most attractive commercial topologies. The basic difference between series resonant converter and LLC converter is the insertion of parallel inductor which maybe the magnetising inductance of the transformer in the bridge converters.

A detailed analysis and an analytical solution for the different modes for the variable frequency LLC resonant converter has been discussed in [5] using time domain methods. Some new applications require LLC converters that can operate over a load range which cannot be practically provided using just variable frequency control. Phase shifted control (PSC) can be combined with variable frequency control [6] to extend the voltage regulation range. The steady state equations for Discontinuous Conduction (DCM) of the PSC LLC converter are discussed in [7,8]. A steady state analysis of the phase shifted LLC converter is performed numerically in [9]. Fourier analysis of phase controlled LLC converter has been published in [10]. However, there is no discussion about the operation modes There is a clear gap within the existing literature with regard to a full analytical approach for PSC LLC converters.

The major contribution of this paper is to present different stages of phase modulated LLC resonant converter. Six operational modes found from a combination of these stages are also discussed.

II. ANALYSIS

The topology of the LLC series resonant converter is shown in Fig. 1. This converter is a three element converter consisting of resonant inductor (L), resonant capacitor (C) and magnetizing inductor (L_M). The input voltage is V_{in} and the output voltage is V_o. The full bridge inverter has four switches (S_1, S_2, S_3, S_4). Secondary side of transformer consists of full bridge rectifier (D_1, D_2, D_3, D_4) and output capacitor (C_o).

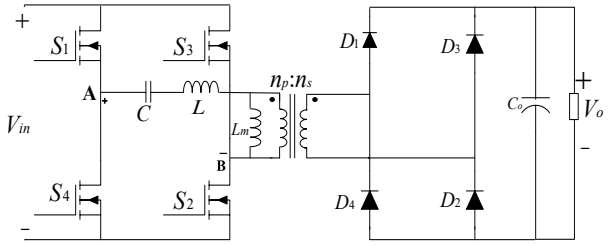

Fig. 1 Full bridge LLC resonant converter

A normalized half period of switching cycle can be defined by,

$$\gamma = \frac{\omega_o}{2f_s} = \frac{\pi}{F} \quad (1)$$

Where, f_s = switching frequency, F= normalized switching frequency.

In a full switching cycle there are twelve switching conditions of primary switches and rectifier diodes which is shown in Table 1. Fig. 2 shows equivalent circuits to model the phase shifted LLC converter over the full period. Due to odd symmetry only six of them are necessary to complete the steady state operation. In equivalent circuits, the amplitude of the input voltage is denoted by $V_1 = V_{in}$ and the output voltage is represented by V_2 which is seen by the resonant network.

To complete the steady state operation in any half cycle, there are a total of six intervals which may or may not occur in every mode.

A. Stage α_1

The primary MOSFETs S_1 and S_2 are turned on and the secondary side current flows through the diodes D_3 and D_4. In this stage, magnetizing inductance does not take part in resonance and it is clamped by output voltage (-V_2). The resonant inductance (L) and the resonant capacitance (C) form the resonant circuit.

TABLE I. DIFFERENT SWITCHING CONDITIONS OF PRIMARY SWITCHES AND RECTIFIER DIODES

Equivalent circuit	(a)	(b)	(c)	(d)	(e)	(f)	(g)	(h)	(i)	(j)	(k)	(l)
$S_1, \overline{S_4}$	ON	OFF	ON	OFF	ON	OFF	OFF	ON	OFF	ON	OFF	ON
$S_2, \overline{S_3}$	ON	OFF	ON	OFF	ON	OFF	ON	OFF	ON	OFF	ON	OFF
D_1, D_2	ON	OFF	OFF	OFF	OFF	ON	ON	OFF	OFF	OFF	OFF	ON
D_3, D_4	OFF	ON	OFF	OFF	ON	OFF	OFF	ON	OFF	OFF	ON	OFF

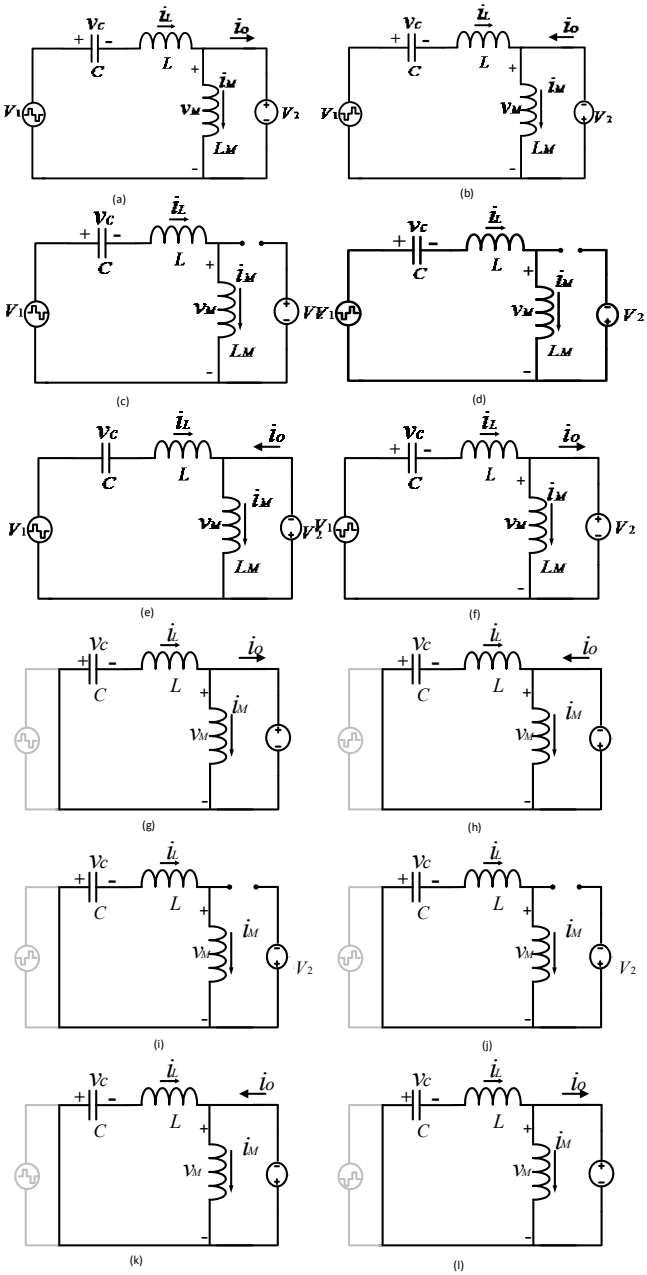

Fig. 2 Equivalent circuits to model the phase shifted LLC converter over full period

The circuit topology for this stage is shown in Fig. 3.

The differential equations of the state variables for this stage are given below,

$$\frac{dv_c}{dt} = \frac{1}{C} i_L \tag{1}$$

$$V_1 = L\frac{di_L}{dt} + v_C - V_2 \tag{2}$$

$$v_M(\omega_o t) = -V_2 \tag{3}$$

$$i_M(\omega_o t) = i_M(0) - \frac{L}{L_M}\frac{V_2}{Z_o}(\omega_o t) \tag{4}$$

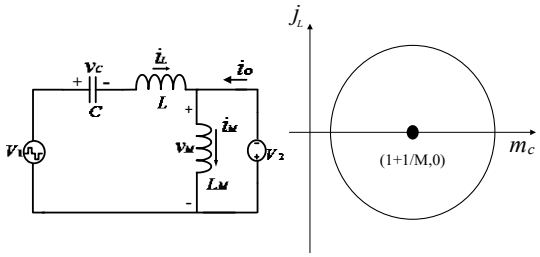

Fig. 3 Circuit topology and corresponding trajectory for stage α_1

Where, v_C and i_L are the instantaneous capacitor voltage and inductor current. By solving equation 2 and 3, the solution of v_C and i_L can be found which is given by:

$$v_C(\omega_o t) = [v_C(0) - (V_1 + V_2)]\cos(\omega_o t) + i_L(0) Z_o \sin(\omega_o t) + (V_1 + V_2) \tag{5}$$

$$i_L(\omega_o t) = i_L(0)\cos(\omega_o t) - \frac{v_C(0) - (V_1 + V_2)}{Z_o}\sin(\omega_o t) \tag{6}$$

Where $v_C(0)$ and $i_L(0)$ are the initial values for resonant capacitor voltage and inductor current, Z_o is the characteristic impedance and ω_o is the resonant frequency of the tank.

$$Z_o = \sqrt{L/C} \tag{7}$$

$$\omega_o = \frac{1}{\sqrt{LC}} = 2\pi f_o \tag{8}$$

Where f_o is the resonant frequency of the LC series circuit.

In this application the output voltage is fixed. Therefore, the output voltage is considered as base quantities. The base quantities are defined by:

$$V_{base} = V_2 = \frac{n_p}{n_s} V_o = \frac{V_o}{n} \tag{9}$$

$$\omega_{base} = \omega_o \tag{10}$$

$$Z_{base} = Z_o = \sqrt{L/C} \tag{11}$$

$$I_{base} = \frac{V_2}{Z_{base}} \tag{12}$$

$$M = \frac{V_2}{V_1} \tag{13}$$

$$\theta = \omega_o t \tag{14}$$

Where, V_o is the output voltage, M is conversion ratio, n_p and n_s are number of transformer primary and secondary

turns, n is the transformer turns ratio and θ is normalized time variable respectively.

The ratio of two inductances is defined by:

$$l = \frac{L}{L_M} \tag{15}$$

To denote normalized voltages and currents lowercase m and j are used respectively and the subscripts of the original variables are retained.

$$m_X(\theta) = \frac{v_X(\theta/\omega_o)}{V_{base}} \tag{16}$$

$$j_Y(\theta) = \frac{i_Y(\theta/\omega_o)}{I_{base}} \tag{17}$$

The final normalized form of steady state solutions of reactive components are given below:

$$m_C(\theta) = (m_C(0) - 1/M - 1)\cos(\theta) + j_L(0)\sin(\theta) + 1/M + 1 \tag{18}$$

$$j_L(\theta) = (-m_C(0) + 1/M + 1)\sin(\theta) + j_L(0)\cos(\theta) \tag{19}$$

$$m_M(\theta) = -1 \tag{20}$$

$$j_M(\theta) = j_M(0) - l\theta \tag{21}$$

Where

$m_C(\theta) =$ Normalized capacitor voltage

$j_L(\theta) =$ Normalized inductor current

$m_M(\theta) =$ Normalized magnetizing inductor voltage

$j_M(\theta) =$ Normalized magnetizing inductor current

The steady state phase trajectory is obtained from equation 19 and 20.

$$(m_C(\theta) - (1/M + 1))^2 + j_L(\theta)^2 = \left(m_C(0) - (\tfrac{1}{M} + 1)\right)^2 + j_L(0)^2 \tag{22}$$

This equation is a circle whose centre is $(1/M + 1,0)$. The radius is a function of the initial conditions of capacitor voltage ($m_C(0)$) and inductor current ($j_L(0)$) and the conversion ratio.

B. Stage α_2

The primary MOSFETs S_1 and S_2 are turned on and the secondary rectifiers are off. No power is flowing to the secondary side. The magnetizing inductance participates in resonance with resonant capacitor and resonant inductor. The Fig. 4 shows the circuit topology and state space trajectory of stage α_2.

The differential equations for the state variables for stage α_2 are given below:

$$\frac{dv_c}{dt} = \frac{1}{C} i_L \tag{23}$$

$$V_1 = L\frac{di_L}{dt} + v_C + L_M\frac{di_L}{dt} \tag{24}$$

$$v_M(\omega_o t) = L_M\frac{di_L}{dt} \tag{25}$$

$$i_M(\omega_o t) = i_L(\omega_o t) \tag{26}$$

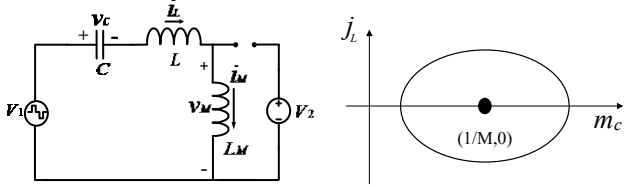

Fig. 4 Equivalent circuit and corresponding trajectory for stage α_2

The solutions of v_C and i_L can be found from equation 24 and 25.

$$v_C(\omega_o t) = [v_C(0) - V_1]\cos(\omega_1 t) + i_L(0)\frac{Z_o}{k_1}\sin(\omega_1 t) + V_1 \tag{27}$$

$$i_L(\omega_0 t) = i_L(0)\cos(\omega_1 t) - (v_C(0) - V_1)\frac{k_1}{Z_o}\sin(\omega_1 t) \tag{28}$$

Where $\omega_1$is the resonant frequency when L_M participates in the resonance. ω_1 is denoted by:

$$\omega_1 = \frac{1}{\sqrt{(L + L_M)C}} \tag{30}$$

$k_1$is the ratio of two resonant frequencies is defined by:

$$k_1 = \frac{\omega_1}{\omega_o} \tag{31}$$

The voltage across the magnetizing inductance can be found by differentiating the inductor current.

The normalized steady state equations for the three reactive components are:

$$m_C(\theta) = \left(m_C(0) - \tfrac{1}{M}\right)\cos(k_1\theta) + \frac{j_L(0)}{k_1}\sin(k_1\theta) + 1/M \tag{29}$$

$$j_L(\theta) = \left(-m_C(\theta_1) + \tfrac{1}{M}\right)k_1\sin(k_1\theta) + j_L(\theta_1)\cos(k_1\theta) \tag{30}$$

$$m_M(\theta) = (\left(-m_C(0) + \tfrac{1}{M}\right)\cos(k_1\theta) - \frac{j_L(0)}{k_1}\sin(k_1\theta))/(1 + l) \tag{31}$$

$$j_L(\theta) = j_M(\theta) \tag{32}$$

The state plane trajectory equation is obtained from equation 32 and 33.

$$(m_C(\theta) - {}^1/_M)^2 + (\frac{j_L(\theta)}{k_1})^2 = (m_C(0) - {}^1/_M)^2 + (\frac{j_L(0)}{k_1})^2 \tag{33}$$

If the same phase plane scales are retained from stage □1, this equation is an ellipse whose centre is $({}^1/_M, 0)$.

C. Stage α_3

The primary MOSFETs S_1 and S_2 are turned on and the secondary side current flows through the diodes D_1 and D_2. In this mode, the magnetizing inductance does not take part in the resonance and it is clamped by output voltage (V_2). The resonant inductance (L) and the resonant capacitance (C) form the resonant circuit. The circuit topology and state space trajectory of stage α_3 are shown in Fig. 5.

The differential equations of the state variables for stage $\alpha_3$are given below:

$$\frac{dv_c}{dt} = \frac{1}{C} i_L \quad (34)$$

$$V_1 = L\frac{di_L}{dt} + v_C + V_2 \quad (38)$$

$$v_M(\omega_o t) = V_2 \quad (35)$$

$$i_M(\omega_o t) = i_M(0) + \frac{L}{L_M}\frac{V_2}{Z_o}(\omega_o t) \quad (36)$$

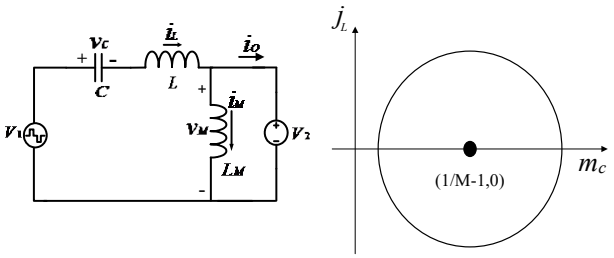

Fig. 5 Equivalent circuit and corresponding trajectory for stage α_3

By solving equation 37 and 38, the solution of v_c and i_L can be found:

$$v_C(\omega_o t) = [v_C(0) - (V_1 - V_2)]\cos(\omega_o t) + i_L(0)Z_o \sin(\omega_o t) + (V_1 - V_2) \quad (37)$$

$$i_L(\omega_o t) = i_L(0)\cos(\omega_o t) - \frac{v_C(0)-(V_1-V_2)}{Z_o}\sin(\omega_o t) \quad (38)$$

The normalized steady state equations of all reactive components for this stage are:

$$m_C(\theta) = (m_C(0) - 1/M + 1)\cos(\theta) + j_L(0)\sin(\theta) + 1/M - 1 \quad (39)$$

$$j_L(\theta) = \left(-m_C(0) + \frac{1}{M} - 1\right)\sin(\theta) + j_L(0)\cos(\theta) \quad (40)$$

$$m_M(\theta) = 1 \quad (41)$$

$$j_M(\theta) = j_M(0) + l(\theta) \quad (42)$$

The trajectory of this stage is obtained from equation 43 and 44.

$$(m_C(\theta) - (1/M - 1))^2 + j_L(\theta)^2 = \left(m_C(0) - (\frac{1}{M} - 1)\right)^2 + j_L(0)^2 \quad (43)$$

This equation is a circle whose centre is at $(\frac{1}{M} - 1,0)$. The radius is a function of stored energy and can be calculated from the initial conditions of resonant inductor current and resonant capacitance voltage and the conversion ratio.

D. Stage α_4

The primary MOSFETs S_2 and S_4 are turned on and the current is flowing to the secondary side through rectifiers D_1 and D_2. In this stage, magnetizing inductance does not take part in resonance and it is clamped by output voltage (V_2). The resonant inductance (L) and the resonant capacitance (C) form the resonant circuit. The circuit topology and state space trajectory of stage α_4 are shown in Fig. 6.

The differential equations of the state variables are given below:

$$\frac{dv_c}{dt} = \frac{1}{C} i_L \quad (48)$$

$$L\frac{di_L}{dt} + v_C + V_2 = 0 \quad (44)$$

$$v_M(\omega_o t) = V_2 \quad (45)$$

$$i_M(\omega_o t) = i_M(0) + \frac{L}{L_M}\frac{V_2}{Z_o}(\omega_o t) \quad (46)$$

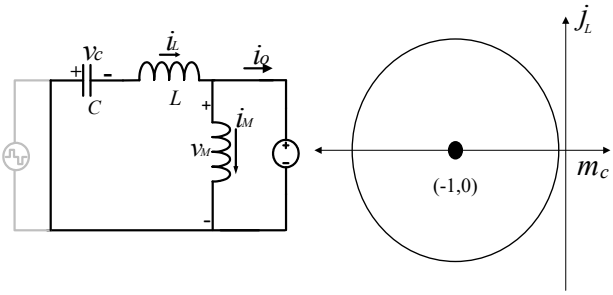

Fig. 1 Equivalent circuit and corresponding trajectory for stage α_4

By solving equation 48 and 49, the solution of v_c and i_L can be found:

$$v_C(\omega_o t) = [v_C(0) + V_2]\cos(\omega_o t) + i_L(0)Z_o \sin(\omega_o t) - V_2 \quad (47)$$

$$i_L(\omega_o t) = i_L(0)\cos(\omega_o t) - \frac{v_C(0) + V_2}{Z_o}\sin(\omega_o t) \quad (48)$$

The normalized steady state equations of the reactive components are:

$$m_C(\theta) = (m_C(0) + 1)\cos(\theta) + j_L(0)\sin(\theta) - 1 \quad (49)$$

$$j_L(\theta) = j_L(0)\cos(\theta) - (m_C(0) + 1)\sin(\theta) \quad (50)$$

$$m_M(\theta) = 1 \quad (51)$$

$$j_L(\theta) = j_M(0) + l(\theta) \quad (52)$$

The trajectory of this stage is obtained from equation 54 and 55.

$$(m_C(\theta) - (-1))^2 + j_L(\theta)^2 = (m_C(0) - (-1))^2 + j_L(0)^2 \quad (53)$$

This equation is a circle whose centre is at (-1, 0).

E. Stage α_5

The primary MOSFETs S_2 and S_4 are turned on and no current is flowing to the secondary side through rectifiers. In this stage the magnetizing inductance participates in resonance with resonant capacitor and resonant inductor. The circuit topology and state space trajectory of stage α_5 are shown in Fig. 7.

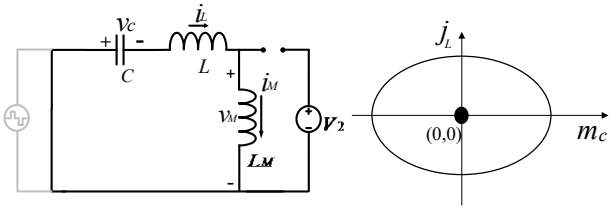

Fig. 2 Equivalent circuit and corresponding trajectory for stage α_5

The differential equations of the state variables for stage α_5 are given below:

$$\frac{dv_c}{dt} = \frac{1}{C} i_L \quad (54)$$

$$L\frac{di_L}{dt} + v_C + L_M\frac{di_L}{dt} = 0 \quad (55)$$

$$v_M(\omega_o t) = L_M\frac{di_L}{dt} \quad (56)$$

$$i_M(\omega_o t) = i_L(\omega_o t) \quad (57)$$

The solutions of v_C and i_L can be found from equation 59 and 60.

$$v_C(\omega_o t) = v_C(0)\cos(\omega_1 t) + i_L(0)\frac{Z_o}{k_1}\sin(\omega_1 t) \quad (58)$$

$$i_L(\omega_0 t) = i_L(0)\cos(\omega_1 t) - v_C(0)\frac{k_1}{Z_o}\sin(\omega_1 t) \quad (59)$$

The normalized steady state equations of the reactive components are:

$$m_C(\theta) = \left(1/k_1\right) j_L(0)\sin[k_1\theta] + m_C(0)cos[k_1\theta] \quad (65)$$

$$j_L(\theta) = j_L(0)cos[k_1\theta] - k_1 m_C(0)\sin[k_1\theta] \quad (66)$$

$$m_M(\theta) = [-m_C(0)cos[k_1\theta] - (1/k_1) j_L(0)\sin[k_1\theta]]/1 + l \quad (67)$$

$$j_L(\theta) = j_M(\theta) \quad (68)$$

The state plane trajectory equation is obtained from equation 65 and 66.

$$(m_C(\theta))^2 + (\frac{j_L(\theta)}{k_1})^2 = (m_C(0))^2 + (\frac{j_L(0)}{k_1})^2 \quad (60)$$

This equation is an ellipse whose centre is (0,0).

F. Stage α_6

The primary MOSFETs S_2 and S_4 are turned on and the current is flowing to the secondary side through rectifiers D_3 and D_4. In this mode, magnetizing inductance does not take part in resonance and it is clamped by output voltage $(-V_2)$. The resonant inductance (L) and the resonant capacitance (C) form the resonant circuit. The circuit topology and state space trajectory of stage α_6 are shown in Fig. 8.

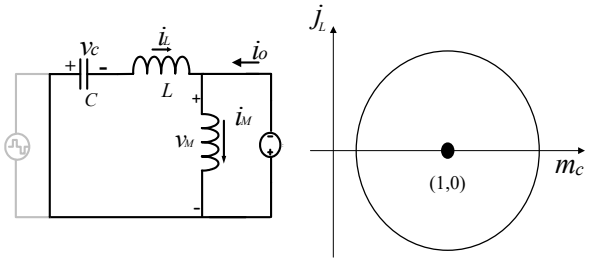

Fig. 3 Equivalent circuit and corresponding trajectory for stage α_6

The differential equations of the state variables are given below:

$$\frac{dv_c}{dt} = \frac{1}{C} i_L \quad (61)$$

$$L\frac{di_L}{dt} + v_C - V_2 = 0 \quad (62)$$

$$v_M(\omega_o t) = -V_2 \quad (63)$$

$$i_M(\omega_o t) = i_M(0) - \frac{L}{L_M}\frac{V_2}{Z_o}(\omega_o t) \quad (64)$$

By solving equation 70 and 71, the solution of v_c and i_L can be found:

$$v_C(\omega_o t) = [v_C(0) - V_2]\cos(\omega_o t) + i_L(0)Z_o\sin(\omega_o t) + V_2 \quad (65)$$

$$i_L(\omega_o t) = i_L(0)\cos(\omega_o t) - \frac{v_C(0) - V_2}{Z_o}\sin(\omega_o t) \quad (66)$$

The normalized steady state equations of the reactive components are:

$$m_C(\theta) = (m_C(0) - 1)\cos(\theta) + j_L(0)\sin(\theta) + 1 \quad (67)$$

$$j_L(\theta) = j_L(0)\cos(\theta) - (m_C(0) - 1)\sin(\theta) \quad (68)$$

$$m_M(\theta) = -1 \quad (69)$$

$$j_L(\theta) = j_M(0) - l(\theta) \quad (70)$$

The trajectory of this stage is obtained from equation 76 and 77.

$$(m_C(\theta) - 1)^2 + j_L(\theta)^2 = (m_C(0) - 1)^2 + j_L(0)^2 \quad (71)$$

This equation is a circle whose centre is at (1, 0).

III. OPERATIONAL MODES

A. Continuous Conduction Mode (CCM I)

The time domain waveforms and the state space trajectory are shown in Fig. 9 (a).

B. Continuous Conduction Mode (CCM II)

The time domain waveforms and the state space trajectory are shown in Fig. 9 (b).

C. Discontinuous Conduction Mode (DCM I)

The time domain waveforms and the state space trajectory are shown in Fig. 9 (c).

D. Discontinuous Conduction Mode (DCM II)

The time domain waveforms and the state space trajectory are shown in Fig. 9 (d).

E. Discontinuous Conduction Mode (DCM III)

The time domain waveforms and the state space trajectory are shown in Fig. 9 (e).

F. Discontinuous Conduction Mode (DCM IV)

The time domain waveforms and the state space trajectory are shown in Fig. 9 (f).

IV. DESIGN GUIDELINE

As there are six modes in phase shifted LLC converter, a designer has to choose the parameters depending on the application. If the application is a fixed load, the CCM I would be the best choice as it would give the highest efficiency. A prototype has been built to deliver 300 W at 30V input and 400V output. At full load the converter falls into CCM I mode. This mode has the highest efficiency as it operates at 50% duty cycle. However, in case of light loads, the converter is more prone to DCM modes. The efficiency curve at different loads showing different modes is shown in Fig. 10. Zero voltage switching of the converter is lost in CCM II and DCM IV modes. Again, in wider voltage ranges, such as solar module application, the converter can be designed at nominal voltage.

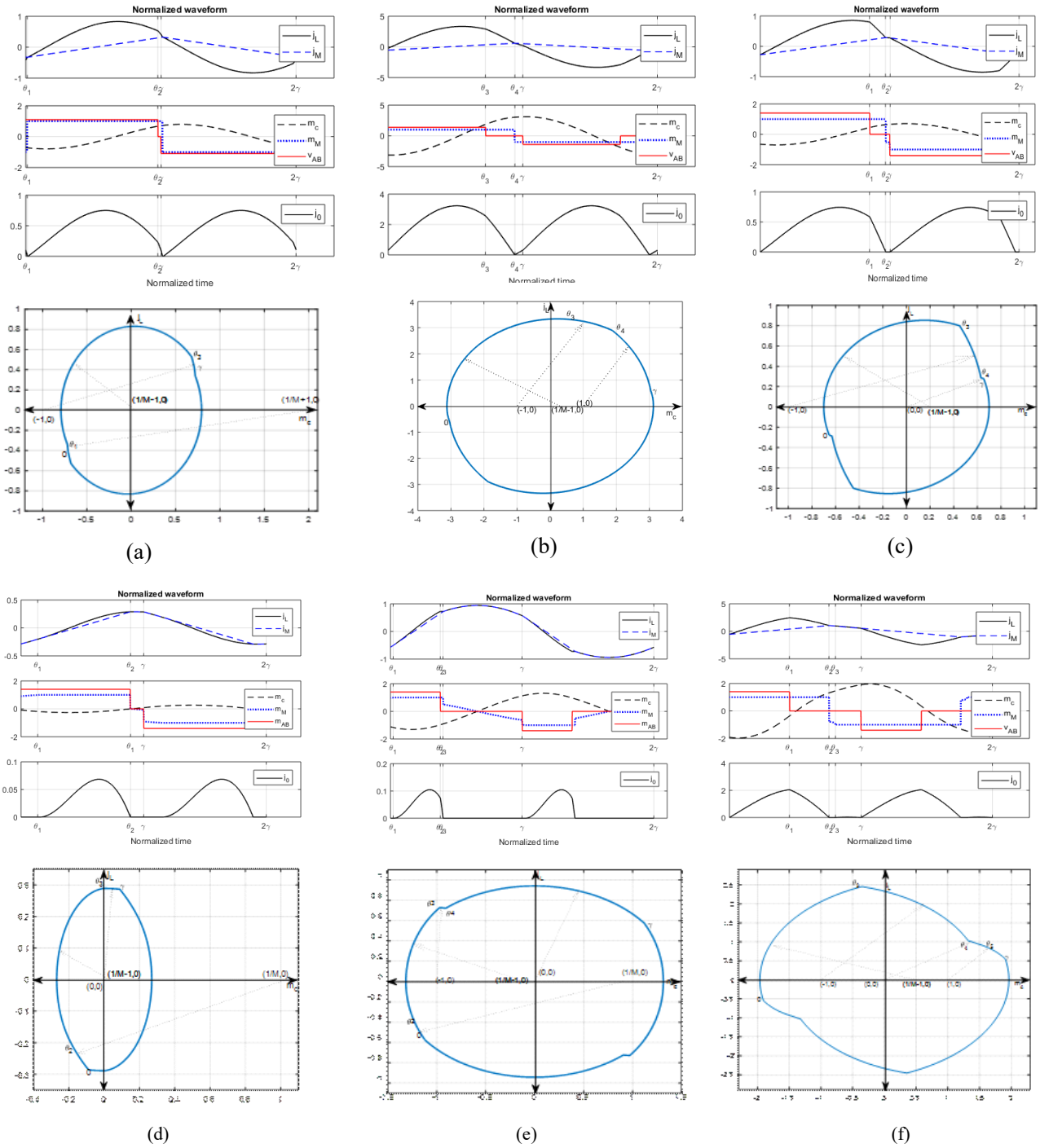

Fig. 9 Steady state time domain waveforms and state space trajectory (a) CCM I (b) CCM II (c) DCM I (d) DCM II (e) DCM III (f) DCM IV

In that case, there is a possibility that the converter switches will lose zero voltage switching at higher voltages and falls into CCM II mode.

V. CONCLUSION

This paper presents a detailed steady state analysis of the operational modes of the phase shifted LLC resonant converter. This analysis was further extended to have analytical solution to each mode. Six operational modes exist. The analysis is done on the normalized form. Time domain waveforms and state plane trajectories are also presented. A design guideline has been presented to choose the best mode from available modes. This would give an insight to the designer to which mode should be chosen depending on the application.

REFERENCES

[1] M. M. JovanoviĆ, "Invited paper. Resonant, quasi-resonant, multi-resonant and soft-switching techniques—merits and limitations," *International Journal of Electronics,* vol. 77, no. 5, pp. 537-554, 1994/11/01 1994.

[2] I. Batarseh, "Resonant converter topologies with three and four energy storage elements," *IEEE Transactions on Power Electronics,* vol. 9, no. 1, pp. 64-73, 1994.

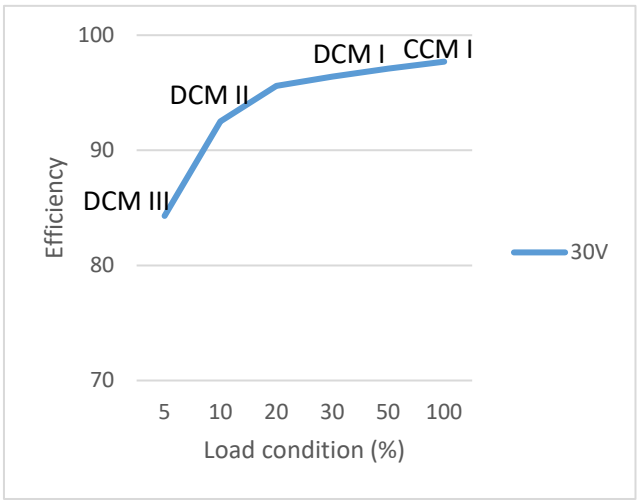

Fig. 10 Efficiency curve for different load at 30V showing the operational modes.

[3] S. Deb, A. Joshi, and S. R. Doradla, "A novel frequency-domain model for a parallel-resonant converter," *IEEE Transactions on Power Electronics,* vol. 3, no. 2, pp. 208-215, 1988.

[4] U. Mumtahina and P. Wolfs, "A comparison study between series resonant and zero-voltage-resonant-transition DC-DC converters," in *2015 Australasian Universities Power Engineering Conference (AUPEC)*, 2015, pp. 1-6.

[5] X. Fang, H. Hu, Z. J. Shen, and I. Batarseh, "Operation Mode Analysis and Peak Gain Approximation of the LLC Resonant Converter," *IEEE Transactions on Power Electronics,* vol. 27, no. 4, pp. 1985-1995, 2012.

[6] S. M. S. I. Shakib and S. Mekhilef, "A Frequency Adaptive Phase Shift Modulation Control Based LLC Series Resonant Converter for Wide Input Voltage Applications," *IEEE Transactions on Power Electronics,* vol. 32, no. 11, pp. 8360-8370, 2017.

[7] J. H. Kim, C. E. Kim, J. K. Kim, J. B. Lee, and G. W. Moon, "Analysis on Load-Adaptive Phase-Shift Control for High Efficiency Full-Bridge LLC Resonant Converter Under Light-Load Conditions," *IEEE Transactions on Power Electronics,* vol. 31, no. 7, pp. 4942-4955, 2016.

[8] H. Wu, X. Zhan, and Y. Xing, "Interleaved LLC Resonant Converter With Hybrid Rectifier and Variable-Frequency Plus Phase-Shift Control for Wide Output Voltage Range Applications," *IEEE Transactions on Power Electronics,* vol. 32, no. 6, pp. 4246-4257, 2017.

[9] W. Liu, B. Wang, W. Yao, Z. Lu, and X. Xu, "Steady-state analysis of the phase shift modulated LLC resonant converter," in *2016 IEEE Energy Conversion Congress and Exposition (ECCE)*, 2016, pp. 1-5.

[10] N. Kollipara, M.K.Kazimierczuk, A.Reatti and F. Corti, "Phase Control and Power Optimization of LLC Converter," IEEE International Symposium on Circuits and Systems (ISCAS), 2019, pp. 1-5.